

# **Two Model Scenarios Illustrating the Effects of Land Use and Climate Change on Gravel Riverbeds of Suburban Maryland, U.S.A.**

Jim Pizzuto  
Department of Geology  
University of Delaware  
Newark, DE 19711

Glenn Moglen  
Department of  
University of Maryland  
College Park, MD

Margaret Palmer  
Director, UMCES Chesapeake Biological Laboratory  
PO Box 38  
1 Williams Street  
Solomons, MD 20699

Karen Nelson  
Department of Entomology  
PLS 4112  
University of Maryland  
College Park, MD 20742-4454

address correspondence to Jim Pizzuto; Fax: 302-831-4158  
Email addresses: [pizzuto@udel.edu](mailto:pizzuto@udel.edu), [moglen@eng.umd.edu](mailto:moglen@eng.umd.edu), [mpalmer@umd.edu](mailto:mpalmer@umd.edu), [karen-nelson@verizon.net](mailto:karen-nelson@verizon.net)

## ABSTRACT

We model two scenarios consisting of 10 years of daily discharges to illustrate the effects of changing land use and climate on gravel riverbeds. The Managed Growth/No Climate Change (MGNCC) Scenario represents minimum effects of land use and climate change, while the Urban Sprawl/ Climate Change (USCC) Scenario represents more extensive effects. We apply our scenarios to a 30 m reach of the Northwest Branch of the Anacostia River. We use downscaled precipitation estimates from the Hadley2 GCM to account for climate change, and use a continuous hydrological model to produce discharge estimates. A sediment transport model, combined with empirical formulae to specify upstream sediment inputs, computes changes in grain size distribution, bedload and suspended material discharge, suspended sediment concentration, the areal fraction of the bed in motion, bed elevation and slope, the silt-clay content of the active layer, and something new: the fraction of exposed bedrock in the active layer. The USCC scenario is characterized by larger and more frequent storm flows than the MGNCC scenario, which in turn create increased bedload and suspended load transport, increased bed mobility, and higher suspended sediment concentrations. The USCC scenario is also characterized by extreme variability in mud and bedrock content of the active layer. Convincing model predictions of the influence of climate and land use changes on gravel river beds will require additional study of 1) upstream sediment supply, 2) mud storage and remobilization in gravel streams, and 3) the controls on exposed bedrock in the active layer.

Keywords: climate change, land use, gravel-bed rivers, sediment, stream ecology

## **1. Introduction**

Changes in climate and land use both have profound effects on rivers (Palmer et al., 2002, Macklin et al., 1992, Leopold, 1968). Climate changes influence precipitation and temperature, two variables that either directly or indirectly control the supply of water and sediment to stream channels. Land use changes, particularly conversion from agriculture to urban land uses, also influence storm discharges and sediment supply (Yorke and Herb, 1978). Because storms and sediment supply represent two of the most significant controlling variables on stream morphology, land use and climate changes are clearly important drivers in fluvial geomorphology.

Driven by the industrial revolution and population growth, anthropogenic influences on stream channels have probably never been greater (Hooke, 2000). These influences are primarily exerted by changes in climate and land use. For example, predictions of global climate change suggest future doubling of atmospheric CO<sub>2</sub>, increases in average temperatures by 2-6 degrees C, and increased variability in precipitation (IPCC 1997). At the same time, agricultural land in developed countries is increasingly being converted to urban and suburban land uses (e.g. Irwin and Bockstael, 2004).

The profound influence of changes in climate and land use on streams has been widely noted, but methods for assessing the effects of these changes are poorly developed. In this study, we describe a preliminary effort to determine, in a specific study area, how these drivers acting together collectively influence the bed characteristics of a gravel bed river. Our study is primarily motivated by the ultimate goal of predicting the ecological effects of changing land use and climate, so we particularly focus on

variables that are important to organisms living in gravel bed streams of our humid temperate study area (though this paper does not explicitly address the connection between hydraulic and sediment transport processes and ecological processes).

This paper is designed to present our approach to modeling these processes and to present the results of modeling specific scenarios that illustrate the *combined* effects of both land use and climate change on gravel river beds. This paper does not address the relative contributions of each driver *separately* to changes in stream bed morphology and composition. A future publication is planned to address this interesting issue.

## **2. Regional Setting**

The Northwest Branch of the Anacostia River provides the field setting for our study. The Northwest Branch has a drainage area of 54.6 km<sup>2</sup>, and it is located northwest of Washington, D.C. in Montgomery County, Maryland (detailed location maps are provided by Moore and Palmer, 2002, Palmer et al., 1992, and Yorke and Herb, 1978). A USGS gaging station at the outlet of the basin has been active since 1924. The watershed is underlain by metamorphic rocks and is of low relief (Hunt, 1974). During the period of gaging, land use in the watershed changed from dominantly agricultural to urban. This change occurred mostly after WWII, with a particularly strong pulse of development in the late 1960s and early 1970s. During this time, peak flows increased significantly and base flows decreased significantly (Beigley and Moglen, 2002). Currently, land use in the watershed consists of 8.6% agriculture, 24.8% forest, and 66.6% urban (Palmer et al., 2002).

### **3. Methods**

The goal of our research is to evaluate the influence of specific land use and climate change scenarios on stream channel bed sediment characteristics in the Mid-Atlantic region. To accomplish this goal, we first defined two scenarios with differing land use and climate characteristics. One scenario we term the “Managed Growth/No Climate Change Scenario (MG/NCC)”, while the other is referred to as the “Urban Sprawl/Climate Change Scenario (USCC)”. These two scenarios reflect extreme end members of possible disturbances to fluvial and stream ecological systems. The MG/NCC scenario reflects relatively modest disturbance from land use changes, and no disturbance from climate changes. The USCC scenario reflects significant disturbances from both land use and climate changes. Our approach involves comparing model predictions of fluvial response to these two scenarios to help clarify the extent of disturbances from a combination of both climate and land use changes.

The Managed Growth / No Climate Change scenario is based on climate data from the years 1960 – 1969. Precipitation is computed using the Hadley 2 Global Circulation Model (GCM) for air temperature, with a year-round average of 17.3 degrees Celsius. Precipitation data were estimated on a daily time step. Furthermore, because the grid spacing of the GCM is very large compared to the study area, a procedure was applied to “downscale” the GCM estimates to a scale more appropriate for this study (Hayhoe et al., 2004). Impervious surface is assumed to be 10%, a value below the thresholds generally associated with ecological impairments associated with urbanization, but high enough to be consistent with a significant, densely-packed urban population (Palmer et al., 2002). Forested land use in the watershed is assumed to be 20%, and the

riparian zone adjacent to the stream is assumed to be forested. This level of forestation would be consistent with an urban population only with careful land use planning (Irwin and Bockstael, 2004). Finally, no construction is assumed to be taking place in the watershed.

The Urban Sprawl / Climate Change scenario is based on climate data from the years 2090 - 2099 from the Hadley 2 GCM. These predictions suggest a year-round average of 21.5 degrees Celsius. Precipitation data for these years was also “downscaled”. Impervious surface is assumed to be 30%, a value well above the thresholds associated with impaired ecological assessments of stream habitat, and consistent with the highest levels of impervious surface found at the most urban sites in the region studied by Palmer et al (2002, 2004). Forested land use is assumed to be 1%, and forested buffers missing. This level of deforestation is seen in some of our most urban sites, although buffers are currently more intact (Palmer et al., 2002). Finally, we assume that 2% of the watershed is under construction in a given year.

### 3.1 Description of the The Sediment Transport Models

#### 3.1.1. Spatial Structure and Definition of Selected Variables

The domain of the model (Figure 1) is represented by a reach of channel of length  $dx$  located within a watershed. The upstream watershed supplies a specified discharge,  $Q$ , during each time step,  $dt$ , in addition to sediment. Sediment is supplied as mud in suspension, and as sand and gravel (additional details are provided below)

The channel is rectangular, and is imbedded in a floodplain of width  $W_f$ . The channel has a bankfull depth  $h_{bf}$ . Within the reach represented by the model, the

floodplain width, bankfull depth, bed and water surface slope ( $S$ ), and channel width ( $W$ ) and rectangular cross-sectional geometry are all constant.

The bed is divided into an active layer of thickness  $L_a$  (Parker, 1991) and a substrate that does not move. Bedrock may intrude into the active layer, and specific “rules” are proposed to govern how bedrock influences bedload transport processes. We have included bedrock in this way because our field observations and those of others (Allmendinger, 2004, Costa 1975) suggest that bedrock strongly influences bed scour and sediment transport processes in our field area.

### 3.1.2. Initial Conditions

Initial values of variables were obtained from field measurements in the study are listed in Table 2. Several of these variables were held constant during the simulations (i.e., the active layer thickness  $L_a$ ). Some initial values, for example, the mud content of the bed, were not measured in the field, and these values were simply assumed to provide starting values for the computations.

### 3.1.3. Boundary Conditions

Boundary conditions are represented by inputs of both water and sediment. Inputs of water are determined using two models, one for precipitation and another to determine water discharge. The supply of sediment is computed using empirical relationships based on extensive field data.

The hydrological model used here, which predicts daily streamflow over the course of the scenarios, is fully described in McCuen and Snyder (1985). The continuous streamflow model used here is consistent in its conceptual structure to the Stanford

Watershed Model (Crawford and Linsley 1966), now commonly used as HSPF (Bicknell et al. 1997). It supports three different forms of runoff production: surface runoff, subsurface runoff, and groundwater runoff. The model requires a daily precipitation and temperature time series as well as parameter values that characterize the land use and underlying geology of the system. In separate studies (Hejazi and Moglgn, 2005, Palmer et al. 2002), we determined the relationships between land use and two important model parameters, namely infiltration versus surface runoff production, and the timing of surface runoff.

Continuous streamflow modeling is tested by visually and quantitatively evaluating goodness-of-fit between simulated and observed streamflow at the site of the USGS stream gages at the outlet of the NW Branch watershed. Measures of goodness of fit include: the correlation coefficient, the Nash-Sutcliff coefficient, the gain coefficient, and the deviation volume. The calibration and other aspects of the hydrologic modeling are discussed in detail by Palmer et al. (2004). Correlation coefficients computed for observed versus computed historical discharges (for example) ranged from 0.49 for the decade of the 1960s to 0.80 for the decade of the 1970s.

Sediment inputs are specified depending on the grain size under consideration. Gravel-sized sediments are supplied that are equal to the capacity of the channel to transport each size fraction at the beginning of each time step. In practice this means that bedload transport equations are used to compute the supply of each size fraction using the sediment and hydraulic characteristics of the model reach at the beginning of each time step. This approach implies that the capacity of the channel and the supply of bed material are always in balance. While this assumption may initially appear unreasonable,

it may be justified because it allows the simulations to proceed without extensive aggradation or degradation of the bed, consistent with field observations in the area (Lewicki, 2005, Costa, 1975).

Sand and silt size fractions are supplied according to empirical functions of land use and water discharge. Suspended sediment concentrations in small watersheds of the study area were extensively studied from 1964-1977 by Yorke and Herb (1978). They measured precipitation, changes in land use, storm discharges and concentrations in a number of watersheds in the region. Although their data represent a limited time span compared to significant periods of climate change, they found that sediment concentrations are strongly influenced by both land use variables and storm flow variables. Here we assume that relationships determined from 1964-1977 can be applied over different time periods, using variables that represent changes in both land use and climate.

First, we obtained a correlation between the peak discharge ratio ( $P_R$ ) and the suspended sediment concentration divided by the percentage of construction in the watershed (raised to a power of 0.3). The peak discharge ratio is

$$P_R = (Q_p - Q_a) / R \quad (1)$$

where  $Q_p$  is the peak discharge during a particular storm,  $Q_a$  is the discharge before the storm, and  $R$  is the total storm runoff. Yorke and Herb (1978) defined by  $Q_a$  as the lowest discharge measured before the rising stage of an individual storm. However, in the modeling studies described below,  $Q_a$  is represented by a constant value equal to the discharge that is equaled or exceeded by 5% of the daily discharge values. To correlate suspended sediment concentration with  $P_R$ , a total of 269 observations were used. The

resulting equation has an  $r^2$  of 0.39 and an F ratio that suggests a “significance” well in excess of 99%. The correlation is strictly an empirical result; the exponent on the percentage of construction of 0.3, for example, was selected solely because it produced acceptable results.

The empirical expression for predicting the suspended sediment concentration,  $C$ , is (Figure 2):

$$C = 1.5 \times 10^{-4} P_c^{0.3} P_R \quad (2)$$

where  $C$  is the concentration by weight of suspended sediment (as a ratio), and  $P_c$  is the percentage of construction in the watershed during the specified time step. In the data set used to establish equation (2), concentrations vary from about  $5 \times 10^{-5}$  to about 0.025, the percentage of construction varies from 0 to about 15%, and the peak ratio varies from 2 to 391.

In order to determine the percentages of sand and mud in suspension, empirical data presented by Yorke and Herb (1978) were used. These authors describe the variation of grain size with discharge for the Anacostia River near Colesville for 1960-1973 in their figure 11 (page 17 of Yorke and Herb, 1978). The percentage of sand increases with increasing discharge, the percentage of silt remains approximately constant at about 45%, and the percentage of clay decreases with increasing discharge.

A simple functional representation of these data would put the % sand ( $P_s$ ) at about 5% for the lowest discharges, and at about 30 % for the highest discharges. In between the lowest and highest discharges, the percentage increases linearly on a plot of % sand as a function of  $\log Q$ . These ideas were quantified using the functions summarized below:

$$\begin{aligned}
P_s &= 0.01 + (5 - .01) * P_R, & P_R < 1 \\
P_s &= 5 + 20.762 * \log_{10}(P_R), & 1 \leq P_R \leq 16 \\
P_{sw} &= 30, & P_R > 16
\end{aligned} \tag{3}$$

These equations are formulated in terms of peak ratio rather than discharge in an effort to produce a non-dimensional empirical equation that could potentially be accurate when applied to watersheds of varying size.

#### 3.1.4. Hydraulic Resistance

The relationship between water depth (H) and discharge was specified using Bray's resistance equation for gravel bed rivers (Chang, 1988). For flows that remained in the channel, this takes the form:

$$h = \left( \frac{K_s^b Q_c}{aW\sqrt{gS}} \right)^{\frac{1}{b+1.5}} \tag{4}$$

where  $Q_c$  is the discharge in the channel,  $h$  is the water depth,  $g$  is the acceleration of gravity,  $K_s$  is a roughness length, and  $a$  and  $b$  are coefficients equal to 1.36 and 0.281, respectively. For overbank flows, three equations must be must be solved by trial for  $h$ :

$$Q_c = \frac{aW\sqrt{gS}}{K_s^b} h^{1.5+b} \quad (5)$$

$$Q_f = \frac{aW_f\sqrt{gS}}{K_{sf}^b} (h - h_{bf})^{1.5+b} \quad (6)$$

$$Q = Q_c + Q_f \quad (7)$$

where  $Q$  is the total discharge,  $Q_f$  is the discharge on the floodplain, and  $K_{sf}$  is the roughness of the floodplain.  $K_s$  was calibrated using measured stage discharge data for the study area at 0.2 m, while  $K_{sf}$  was arbitrarily set at 0.02 m for all computations (Table 2)(i.e. no attempt was made to adjust  $K_{sf}$  for the presence or absence of forested riparian zones)..

### 3.1.5. Representation of the Bed

The bed in the model consists of mud, sand, gravel, and bedrock in deposits that lie below the sediment-water interface. The bed itself is divided into an active layer of thickness  $L_a$  in which bed material transport is localized (Parker, 1991). The active layer is considered to be “well-mixed” (i.e., grain size distribution and bed porosity are treated as being uniform through the active layer). The numerical value of the active layer thickness is presented as an input parameter in the simulation, and it does not vary with time, flow conditions, or the grain size of the bed (a value of 0.1 m was used to obtain the results in this paper).

The material in the active layer is divided into three different constituents: sand and gravel, bedrock, and mud. The grain size distribution of sand and gravel is specified by denoting the fractions,  $f_i$ , of specified sizes present on the bed. These fractions specifically include the fraction of bedrock exposed in the active layer. As a result, all sand and gravel grain size fractions and the fraction of bedrock must sum to 1.

Mud in the bed is treated somewhat differently. The sand and gravel in the active layer is assumed to have a constant porosity. The pores in the sand and gravel are then available to be filled with mud. If the pores in the active layer become completely filled with mud, mud may be deposited on top of the active layer of sand and gravel if hydraulic conditions permit this to occur (mud transport processes are described in greater detail below).

### 3.1.6. Bedload Transport, Bed Mobility, and Changes in Bed Material Grain Size Distribution

Bed load transport rates are computed using the equations of Wilcock and Crowe (2003). Transport rates are determined for specified size fractions from sand to gravel. In this paper, 3 sand size fractions and 7 gravel size fractions from granule to boulders are computed.

The areal extent of bedload transport,  $A_t$ , is an important parameter for stream ecology, and therefore the model estimates this parameter also. Methods of Wilcock (1997) are used to determine the areal extent of bed material transport at each time step. If otherwise not specified, the coefficients required by these methods are taken directly from Wilcock's (1997) laboratory studies.

Changes in the bed material grain size fractions of the active layer,  $F_i$ , were computed using a modified version of the approach proposed by Parker (1991):

$$(1 - \lambda_p) \left[ L_a \frac{\partial F_i}{\partial t} + (F_i - f_{li}) \frac{\partial L_a}{\partial t} \right] = - \frac{\partial q_{bi}}{\partial x} + f_{li} \frac{\partial q_{bT}}{\partial x} \quad (8)$$

where  $\lambda_p$  is the porosity of the bed,  $t$  is time,  $x$  is the downstream spatial coordinate,  $q_{bi}$  is the volumetric bed material transport rate of grain size fraction  $i$ ,  $q_{bT}$  is the total volumetric bed material transport rate (i.e.,  $q_{bi}$  summed over all grain sizes), and  $f_{li}$  is the fraction of grain size  $i$  at the interface between the active layer and the substrate. The value of  $f_{li}$  is set equal to 0 if the fraction of the bedrock ( $F_{brf}$ ) in the active layer is positive. If  $F_{brf} = 0$ , then methods of Parker are used to determine  $f_{li}$ . During periods of bed aggradation and degradation, sediment transfers between the load, substrate, and the active layer are computed using the weighted average approach described by Cui et al. (1996).

### 3.1.7. Changes in the Fraction of Bedrock in the Active Layer

If equation (8) is rederived with bedrock as a constituent of the active layer, and if the resulting equation is summed over all grain sizes, then equation (9) is obtained:

$$(1 - \lambda_p) \frac{\partial L_a}{\partial t} (f_{brfl} - F_{brf}) - (1 - \lambda_p) L_a \frac{\partial F_{brf}}{\partial t} + (1 - \lambda_p) (1 - f_{brfl}) \frac{\partial \eta}{\partial t} = - \frac{\partial q_{bT}}{\partial x} \quad (9)$$

where  $f_{brfl}$  is the bedrock fraction at the interface between the substrate and the active layer. According to equation (9), the presence of bedrock in the active layer results in an interesting set of possibilities when gradients in total bedload transport exist. For

example, an excess of supply over transport capacity could result in sediment storage in the reach. Equation (9) suggests that this storage could be accommodated in one of 3 possible ways: 1) deposition on the bed (i.e., positive  $(\partial\eta/\partial t)$ , 2) a decrease in bedrock fraction in the active layer (i.e., negative  $\partial F_{brf}/\partial t$ ), or 3) changes in the thickness of the active layer, modulated by a difference between the bedrock fraction in the active layer and that at the boundary of the substrate (first term on the left of equation (9))(this third option, of course, was not explicitly considered during this study because  $L_a$  is treated as a constant during the present simulations).. It is important to note that current understanding of partially alluvial channels is not sufficient to predict which of these three outcomes will occur, or if a some combination of the three is likely.

In the absence of a clear understanding of how to “partition” sediment transport gradients between the three terms on the left of equation (9), several “rules” are adopted here. First, it is assumed that the thickness of the active layer,  $L_a$ , remains constant during the simulation. This removes the first term on the left of equation (9). Second, it is assumed that when  $F_{brf} > 0$ , imbalances in sediment flux are accommodated by changes in bedrock fraction (i.e., the middle term on the left of equation (9)) rather than by changes in the elevation of the bed. It is only when the channel becomes fully alluvial, i.e., when  $F_{brf} = 0$ , that gradients in bedload transport are accommodated by changes in bed elevation.

The arbitrary nature of these rules should be noted. Further studies, presumably in the laboratory, are urgently needed to better define how gradients in sediment transport lead to changes in bed elevation and the fraction of bedrock in the active layer.

Equation (9) is not actually implemented in the numerical model – it is presented here to clarify the rules used to determine changes in  $F_{brf}$ .  $F_{brf}$  is actually computed by summing all the other grain size fractions,  $F_i$ , during a time step (after these have been determined by solving equation (8), and noting that all of the grain size fractions AND the bedrock fraction must sum to 1.

### 3.1.8. Computing Washload Concentrations

The washload concentration  $C_m$  is determined by solving a mass balance equation of suspended fine grained sediment. This equation is:

$$\frac{\partial(hC_m)}{\partial t} = -\frac{1}{W} \frac{\partial(QC_m)}{\partial x} - D(\tau) + E(\tau) \quad (10)$$

where  $W$  is the channel width and  $D$  and  $E$  are rates of deposition and erosion of mud, respectively. Both  $D$  and  $E$  have units of volume of mud eroded per unit bed area per unit time ( $m^3/m^2/t$ ).

### 3.1.9. Specifying Rates of Erosion and Deposition of Mud on the Bed

Storage of “fine” sediment in gravel river beds has been investigated in the field and laboratory (Rehg et al., 2005, Packman and McKay, 2003, Carling, 1984, Diplas and Parker, 1992, Jobson and Carey, 1989, Lisle, 1989, Reid and Frostick, 1985, Frostick et al., 1984, and many others). These studies have indicated that a variety of variables control the extent of storage and remobilization of fine-grained sediment, including the

grain size distributions of the bed and the “fines”, the concentration of fine-grained sediment in transport, the chemical properties of the fine-grained sediment, the extent and intensity of bed material transport, the nature of hyporheic exchange between the flow and the bed, and the bed topography viewed at a variety of spatial scales. In some cases, deposition of fine-grained sediment is concentrated in a thin surface layer of the bed, while in other cases, deposition occurs to considerable depth within the bed material. Surface layers of fine-grained sediment may be observed on the bed under certain conditions, while deposition is limited to the interstitial openings under other conditions. The definition of “fine” sediment is particularly broad, and often includes sand sizes in addition to silt and clay. General, quantitative models to evaluate storage and remobilization of mud in gravel beds are lacking.

Because the processes of fine-grained sediment erosion and deposition over gravel beds are poorly understood, and to produce a relatively simple model that does not require a large number of unknown parameters, a series of “rules” are followed here to represent these processes. Rates of deposition and erosion are specified as simple functions of the bed shear stress,  $\tau$ :

$$D = C_m V_s(\tau) \quad (11)$$

$$E = E(\tau) \quad (12)$$

where  $V_s(\tau)$  is the settling velocity of mud.  $V_s$  is specified as:

$$V_s = 0, \quad \tau > \tau_{cd} \quad (13)$$

$$V_s = V_{ss} \quad \tau \leq \tau_{cd} \quad (14)$$

here  $\tau_{cd}$  is a critical boundary shear stress for mud deposition (Partheniades, 1986), and  $V_{ss}$  is the settling velocity of mud sized sediment under conditions of deposition.

Deposited sediment can be stored in two places in the bed. If the pores of the active layer are not completely filled with mud, then the volume of mud deposited during a time step can be placed in the pores. If the pores are completely filled (either by previous deposition, or by part of the mud deposited during a current time step), then mud is deposited on top of the sand and gravel active layer as a layer of pure mud (i.e., mud without any sand and gravel within it).

The erosion rate  $E(\tau)$  is given by:

$$E = V_{me} / \Delta t \quad (15)$$

where  $V_{me}$  is the volume of mud eroded per unit bed area during a particular time step.

The volume of mud eroded is determined by a series of rules. If a layer of mud is present, and if the boundary shear stress exceeds a critical threshold for mud erosion  $\tau_{ce}$ , then the entire mud layer is removed, and this volume contributes to  $V_{me}$ .

If gravel is in motion, mud can also be removed from the pores of the active layer. Mud is removed from pores when the fraction of pores filled with mud is greater than the total fraction of the active layer that is NOT immobile. This implies that the portion of the gravel layer without mud in its pores is moved first. If, however, some fraction of the active layer is in motion that contains mud, all the mud in these pores is moved during a time step.

These rules lead to the following quantitative expressions for the solid volume of mud removed from the bed during a time step:

$$V_{me} = V_{ms} + V_{mp} \quad (16)$$

where  $V_{ms}$  is the volume of the surface layer of mud removed (if any)(per unit bed area) and  $V_{mp}$  is the volume of mud per unit bed area eroded from pores.  $V_{ms}$  and  $V_{mp}$  are specified by

$$V_{ms} = T_s(1 - \lambda_m) \quad (17)$$

$$V_{mp} = f_c L_a(1 - \lambda_m) \quad (18)$$

where  $T_s$  is the thickness of the mud layer,  $\lambda_m$  is the porosity of the mud deposit, and  $f_c$ , the fraction of the active layer “cleaned” by erosion, is given by:

$$f_c = 0 \quad A_t \leq f_{pm} \quad (19)$$

$$f_c = A_t - f_{pm}, \quad A_t > f_{pm} \quad (20)$$

where  $f_{pm}$  is the fraction of the pores filled with mud at the beginning of the current time step.

### 3.1.10. Numerical Methods and Programming

The two differential equations presented above (Equations 8 and 10) are discretized using simple explicit finite different approximations. The program is written as a MATLAB script and executed in MATLAB version 5.2. A spatial step of 30 m was used in all computations. The time step was varied to insure accuracy and numerical stability. For the lowest flows, a time step of 3000s proved adequate. For higher flows, the time step was decreased stepwise with increasing discharge in 4 steps to a minimum value of 60s.

### 3.2. Sensitivity Analysis

Because many of the parameters required by the model are poorly constrained by either field observations or even scientific understanding, we performed a sensitivity analysis to document how our results might be influenced by uncertainty in estimating input variables and parameters. The sensitivity analysis was based on a two-year

simulation of daily flows using the USCC scenario. Independent variables selected for sensitivity analysis included input values of the daily discharge  $Q$ , the thickness of the active layer  $L_a$ , the roughness length of the channel bed  $K_s$ , the bed porosity  $\lambda_p$ , the critical shear stress for mud deposition (and erosion)  $\tau_{cd}$ , the concentration of suspended sediment supplied by from the watershed  $C$ , and the volume of bed material supplied by the watershed for each grain size fraction  $q_{bi}$ . During the sensitivity analysis, each of these independent variables was increased by 50% from “base” values used in the USCC simulation (the volume of bed material, however, was decreased by 50% because of numerical issues that arose when the model was run using increased bedload transport rates). For variables such as discharge that change with each day of the simulation, all the daily values were increased (or decreased) by 50%. For each independent variable, model sensitivity was assessed by computing mean and 90<sup>th</sup> percentiles for the 730 daily values of 4 dependent variables: the fraction of exposed bedrock in the active layer ( $F_{brf}$ ), the areal fraction of the bed mobilized, the fraction of mud filled with pores ( $f_{pm}$ ), and the concentration of suspended wash load  $C_m$ . Differences between the “base” simulation and the simulations obtained by varying individual parameters were expressed as % differences according to the following formula:

$$\% \text{ difference} = 100 * (\text{statistic from sensitivity simulation} - \text{statistic from base simulation}) / (\text{statistic from base simulation}) \quad (21)$$

where the “statistic” in equation (21) could refer to either the median or the 90<sup>th</sup> percentile value for the parameter in question.

#### 4. Results

The total precipitation varied considerably between the MGNCC and the USCC scenarios. For the MGNCC scenario, a total of 2601 mm occurred in the 10 year period between 1960 and 1969. For the USCC scenario, a total of 3193 mm occurred from 2090 and 2099.

The greater precipitation estimated for the USCC scenario is reflected in flow duration curves of daily discharges obtained from hydrological modeling (Figure 3). Only the upper ends of the flow duration curves are illustrated in Figure 3, because at lower durations, the two curves are indistinguishable. This indicates that the USCC scenario is characterized by higher storm flows than the MGNCC scenario. It is useful to note that discharge in Figure 3 is illustrated on a logarithmic axis, so the storm flows for the USCC scenario are substantially larger than those of the MGNCC scenario.

The increased storm discharges of the USCC are not surprisingly reflected in increased volumes of bedload transported out of the study reach during the 10 year simulation period. The results of the simulations (not presented here due to space limitations) indicate that the total volume of bed material transported under the USCC scenario is more than two times the volume transported under the MGNCC scenario. Furthermore, most of the sediment is transported during 6 or 7 large storms.

“Duration” curves illustrating the areal fraction of the bed that is mobile during transport events for the two scenarios are illustrated in Figure 4. Not surprisingly, the larger floods of the USCC scenario are associated with greater areal bed mobility than the MGNCC scenario. At a duration of 50%, for example, the USCC scenario predicts about 65% areal bed mobility, while the MGNCC scenario is associated with about 62% areal

bed mobility. The maximum bed mobility for the USCC scenario is about 83%, while that for the MGNCC scenario is about 76%. Box plots inset into Figure 4 illustrate the distributions of bed mobility for the MGNCC and USCC scenarios (outliers, however, are omitted). A non-parametric Kruskal-Wallis analysis yields a p value of less than 0.001, suggesting that the median values of these distributions are significantly different.

The dynamics of the bedrock fraction of the active layer are very different for the two scenarios (Figure 5). For the MGNCC scenario, the exposed bedrock fraction gradually increases during the 10 year simulation from about 2.8% to about 8%, reflecting a reduced sediment transport supply relative to the sediment transport capacity of the stream that is likely related to the current condition of this urbanized watershed. For the USCC, the exposed bedrock fraction varies rapidly between about 0% and 12%, apparently reflecting extremes of supply and transport capacity during the largest floods. However, for most of the time, the bedrock fraction of the active layer during the USCC simulation is lower than that of the MGNCC simulation.

Initial and final grain size frequency curves for the two scenarios are surprisingly similar for the two scenarios (though the details are not presented here). Results are obtained for fine sand up to boulders 500 mm in diameter. Grain size frequency curves for both scenarios suggest considerable changes in bed material grain size distribution during the 10 year simulations. These changes involve a reduction in the fraction of sand sizes on the bed, as well as a reduction in the fractions of the very largest particles on the bed. Remarkably, both scenarios present very similar grain size distributions at the ends of the simulations.

Not surprisingly suspended sediment concentrations for the USCC scenario are significantly higher than those of the USCC scenario, reflecting the greater sediment supply associated with storms in the USCC scenario (Figure 6). ). A non-parametric Kruskal-Wallis analysis of these distributions yields a p value of less than 0.001, suggesting that the median values of the suspended sediment concentrations are drawn from significantly different populations.

The fractions of the active layer filled with mud are compared for the two scenarios in Figure 7. This parameter hovers around 40% for the MGNCC scenario, with occasional excursions from 65% to lows of 20-30%. For the USCC scenario, much greater variability is encountered, with high values of 100% occurring approximately 7 times, and a series of low values of less than 20% occurring a similar number of times. Average values for the USCC scenario appear similar to those of the MGNCC scenario.

Results of sensitivity analyses are presented in Figure 8, where percent differences between the base simulation and simulations with 50% changes to 7 parameters are tabulated. Shading indicates 4 categories of sensitivity, from very low (white) to very high (black). The model appears to be very insensitive to uncertainty in the thickness of the active layer, the roughness length, and the bed porosity. The model is moderately sensitive to changes in discharge. For example, the fraction of bedrock increases when all the discharges are increased by 50% due to scour of the bed, and the 90<sup>th</sup> percentile fraction of pores filled with mud also decreases, presumably due to the same process. However, bed mobility and wash load concentration are insensitive to changes in discharge.

Two independent variables,  $\tau_{cd}$ , and the concentration of suspended sediment supplied from the watershed represent variables that specifically represent fine-grained sediment dynamics in the model. Not surprisingly, variations in these parameters do not influence the bedrock fraction of the active layer or bed mobility. The fraction of pores filled with mud and the concentration of wash load are, however, moderately influenced by changes in these parameters, particularly in the extremes of the distributions represented by the 90<sup>th</sup> percentile statistics.

Remarkably, the model results prove to be most sensitive to the volume of bed material supplied from the watershed. All of the dependent variables show considerable sensitivity to bed material supply. This sensitivity to the imposed decrease of 50% arises because the lack of sediment at all discharges results in scour of the bed, which 1) increases the fraction of exposed bedrock in the active layer, 2) coarsens the bed, thereby reducing bed mobility, 3) replaces unfilled pores with bedrock, increasing the fraction of pores filled with mud, and 4) increases wash load concentrations by scouring mud-filled porous sediment from the bed.

## **5. Discussion**

### **5.1. Interpretations of the Results**

The results presented above can be divided into two categories. One set of results may be derived directly from the higher discharges associated with the USCC scenario. Not surprisingly, these include increased bedload transport, increased bed mobility, and increased suspended sediment concentrations. All of these results are easily associated with higher discharges. The other set of results includes the increased variability in mud and bedrock fractions in the active layer. These results are caused by variations in the

balance between sediment supply and transport capacity, although the detailed mechanisms involved differ somewhat.

The increased variability in mud content of the active layer arises from two related phenomena. First, storm discharges are associated with significantly higher sediment concentrations in the USCC scenario as compared to the MGNCC scenario due to the higher percentage of construction in the USCC scenario (i.e. Equation 2). Flows smaller than the largest stormflows (for example, those in Figure 3 with a duration of about 0.97) occur much more frequently in the USCC scenario, and they carry more sediment than similar duration flows of the MGNCC scenario. At these flows, however, hardly any of the bed is in motion, and therefore extensive amounts of mud are free to accumulate in the pores. Then, when the highest storm flows do occur, nearly all of this mud is removed as most of the active layer is mobilized. This leads to very high levels of variability in mud content of the active layer in the USCC scenario. In the MGNCC scenario, mud accumulates to a lesser degree because of the lower concentrations (Equation (2)), and the extent of erosion is also less because of the reduced mobility of the bed (Figure 4). Both of these processes lead to lower variability in mud content in the MGNCC scenario.

Variability in bedrock fraction arises from changes in the balance between upstream sediment supply and channel transport capacity during the hydrographs of individual storms. First, it is important to realize that the continuous hydrological model predicts that storms last for several days. Thus, each “high flow event” actually consists of a complete hydrograph with rising and falling limbs that involves a number of daily flows. When model predictions are carefully analyzed for individual storm hydrographs, the

following processes are revealed. During the initial rapid rise of flow to the peak discharge of the storm, sediment transport capacity is greater than upstream sediment supply, and as a result, sediment is removed from the active layer, and the fraction of bedrock in the active layer rapidly increases. However, during the falling limb of the storm, the relationship between capacity and supply is reversed, such that supply exceeds capacity, causing sediment to accumulate and the bedrock fraction to gradually decrease. Because both sediment supply and capacity increase significantly during high flows, these imbalances between supply and capacity cause large changes in bedrock exposure during the largest storms. As a result, the larger storm flows of the USCC scenario cause much larger variability in bedrock fraction of the active layer than the somewhat smaller storm flows of the MGNCC scenario.

## 5.2 Implications for Modeling Geomorphic and Ecological Consequences of Climate and Land Use Changes

The results presented above highlight important areas where additional research is needed to provide an improved capability for predicting the responses of river beds to climate changes. These include 1) better methods to predict upstream sediment supply, 2) improved understanding of the partitioning between deposition, erosion, and bedrock exposure of the active layer, 3) better models of wash load storage in river channels, and 4) extension of the model to include channel widening and floodplain accumulation.

It is significant that differences in variability in mud and bedrock fractions in the active layer both arise from the interactions between sediment supply from upstream and transport capacity of the channel. It is also significant that this variability is very important for ecological processes (particularly the mud content of the active layer)(e.g.

Wood and Armitrage, 1997). However, this variability arises from subtle relationships between supply and transport capacity that are rather poorly constrained. The equations for upstream supply of suspended sediment have extremely large amounts of scatter themselves, as is typical of suspended sediment data. Upstream supply of gravel is essentially arbitrarily determined by the capacity of the flow, a “rule” that was adopted in this study primarily because a more convincing approach is unavailable. Because the substantial variability in mud and bedrock content is caused by subtle variations in supply and transport capacity, and because supply in particular is poorly known, one wonders if the model results simply reflect an arbitrarily and poorly constrained knowledge of sediment supply, rather than a well-constrained prediction. Further study of sediment supply processes is clearly important and should be a high priority, particularly given the sensitivity of the computations to assumptions and parameter values that control the supply of suspended sediment and bed material (Figure 8).

The computation of the fraction of bedrock in the active layer is also based on some rather arbitrary rules. These rules are used to determine whether deposited sediment is used to increase the elevation of the bed or to cover exposed bedrock. In the present study, deposition covers bedrock until the bedrock content of the active layer falls to zero. When bedrock is no longer present in the active layer, then increases in bed elevation are allowed. These rules, however, are essentially arbitrary, and other “rules” are possible and even likely. A careful flume study of these processes would be particularly useful in guiding further development of models of “partially alluvial” rivers.

Storage of mud in the pores of the bed is a particularly important ecological process. However, this process has not been extensively studied, and as a result a simple

approach has been adopted in this paper. However, a more convincing method would be desirable, particularly given the sensitivity of mud pore storage processes in the model to sediment supply parameters that are themselves poorly constrained and understood.

The model used in this paper essentially only includes processes that occur on the bed of the stream. However, field observations indicate that the decadal sediment budget of these stream channels is influenced by floodplain accumulation and channel widening (Allmendinger, 2004). A more complete model would also include these processes.

### 5.3 Assessment of Model Results

Given the limitations of the present models discussed above, how should the model results presented in this paper be viewed? Are some of the results robust and convincing, and if so, which ones?

The predictions related to increased storm flows are probably convincing results of climate change and urban sprawl. These include increased suspended sediment concentrations, increased bed mobility, and increased transport of bed material downstream. However, the predictions presented here should be viewed as qualitative trends, rather than as absolute numerical predictions, because the models used here have not been directly calibrated for field conditions.

Other predictions should be evaluated with some caution. The predicted grain size composition of the bed appears to be relatively insensitive to land use and climate changes; however, these computations require accurate prediction of transport of individual size fractions ranging from sand to boulders, and these computations are typically not very precise. Predictions that result from the balance between sediment transport capacity and upstream supply (for example, mud and bedrock content of the

active layer) are also subject to high uncertainty, and the sensitivity analysis clearly indicates that many model predictions are very sensitive to variations in the supply of wash load and bed material. Thus, many of these results should be viewed as hypotheses that require additional testing and model development before being accepted with confidence.

## **6. Conclusions**

In this paper we have reported model results for two scenarios of combined land use and climate change. The models are designed to predict changes in bed elevation, slope, grain size distribution, bedrock exposure, and sediment transport processes for a study area of the Northwest Branch of the Anacostia River in Montgomery County, Maryland, just northwest of Washington D.C. The models provide input for predicting the effects of land use and climate change on stream ecology, so particular attention was given to variables of interest to stream ecologists. The two scenarios reflect end members of 1) minimum disturbance due to land use and climate change (the Managed Growth/No Climate Change scenario) and 2) maximum disturbance (the Urban Sprawl/Climate Change scenario).

The model results indicate that the USCC scenario is associated with larger, more frequent storm discharges than the MGNCC scenario. The increased storm discharges of the USCC scenario create increased bed material transport and bed disturbance, and higher suspended sediment concentrations than those of the MGNCC scenario. Furthermore, the USCC scenario is also associated with highly variable mud and bedrock contents in the active layer. This variability is created by changes in the balance between sediment supply and transport capacity that occur during individual storm hydrographs.

The mud content of the active layer is particularly important for a variety of ecological processes.

Several important processes represented by our models should be studied in greater detail. These include 1) processes that deposit and erode mud from the active layer of the bed, 2) the influence of bedrock on sediment transport and storage in a reach, and 3) processes that supply sediment of all grain sizes to a reach. Future models that represent similar processes on decadal timescales should also include changes in channel width and overbank sedimentation.

## **7. Acknowledgements**

Funding and support for this project was provided by the U.S. Environmental Protection Agency, including the STAR (Science to Achieve Results) Program (EPA Number: R828012) and the Global Climate Change Program (EPA numbers: 1W0594NAEX and R83038701). Two anonymous reviewers provided very helpful comments.

## 8. References

- Allmendinger, N. 2004. The influence of convex-bank floodplains on stream channel processes and morphology in the Mid-Atlantic Piedmont. Ph.D. Thesis, U. of Delaware, Newark, DE, 223 p.
- Beighley, R.E., and G.E. Moglen, 2002. Assessment of stationarity in rainfall-runoff behavior in urbanizing watersheds. *Journal of Hydrologic Engineering*, Am. Soc. Civil Engineers, 7, 27-34.
- Bicknell, B.R., Imhoff, J.C., Kittle, J.L., Donigan, A.S., and Johanson, R.C. 1997. Hydrologic Simulation Program – Fortran. User's Manual for Version 11. EPA/600/R-97/080, E.S. EPA, Ecosystems Research Division, Environmental Research Laboratory, Athens, GA.
- Carling, P.A. 1984. Deposition of fine and coarse sand in an open-work gravel bed. *Canadian Journal of Fisheries and Aquatic Sciences*, 41, 263-280.
- Chang, H., 1988. *Fluvial Processes in River Engineering*. John Wiley, NY. 432 p.
- Costa, J. 1975. Effects of agriculture on erosion and sedimentation in the Piedmont Province, Maryland. *Geological Society of America Bulletin*. 86,1281-1286.
- Crawford, N.H., and Linsley, R.K. 1966. Digital simulation in hydrology: Stanford Watershed Model IV. Stanford University, Department of Civil Engineering Technical Report 39.
- Cui, Y., Parker, G., and Paola, C. 1996. Numerical simulation of aggradation and downstream fining. *Journal of Hydraulic Research*. 34,185-204.

- Diplas, P., and Parker, G., 1992. Deposition and removal of fines in gravel-bed streams, In: Billi, P., Hey, R.D., Thorne, C.R., and Tacconi, P.(Eds.), Dynamics of Gravel-Bed Rivers. John Wiley, London, pp. 313-329.
- Frostick, L.E., Lucas, P.M., and Reid, I., 1984. The infiltration of fine matrices into coarse-grained alluvial sediments and its implications for stratigraphical interpretations. *Journal of the Geological Society of London*. 141, 955-965.
- Hayhoe, K, Cayan, D, Field, C.B., Frumhoff, P.C., Maurer, E.P., Miller, N.L., Moser, S.C., Schneider, S.H., Cahill, K.N., Cleland, E.E, Dale, L., Drapek, R., Hanemann, R.M., Kalkstein, L.S., Lenihan, J., Lunch, C.K., Neilson, R.P., Sheridan, S.C., Verville, J.H., 2004. Emission pathways, climate change, and impacts on California. *Proceedings of the National Academy of Sciences*. 101, 12422-12427.
- Hejazi, M.I., and G.E. Moglen, (in review). The effects of climate and land use change on flow duration in the Maryland Piedmont.” *Journal of Water Resources Planning and Management, American Society of Civil Engineers*.
- Hooke, R.L., 2000. On the history of humans as geomorphic agents. *Geology*. 28, 843-846.
- Hunt, C.B., 1974. *Natural regions of the United States and Canada*. San Francisco, Freeman, 725 pp.
- International Panel on Climate Change, 1997. *The Regional Impacts of Climate Change: An Assessment of Vulnerability*. Watson, R.T., M.C. Zinyowera, and R.H. Moss (Eds.), Report of the IPCC Working Group II Cambridge University Press, Cambridge and New York, 517pp.

- Irwin, E. and Bockstael.,N, 2004. Land use externalities, open space preservation, and urban sprawl. *Regional Science and Urban Economics*. 34, 705-725.
- Jobson, H.E., and Carey, W.P., 1989. Interaction of fine sediment with alluvial streambeds. *Water Resources Research*. 25, 135-140.
- Leopold, L.B., 1968. Hydrology for urban land planning: a guidebook on the hydrologic effects of urban land use. U.S. Geological Survey Circular 554, 18 p.
- Lewicki, M, 2005. A watershed scale numerical model of the impact of land use change on bed material transport in suburban Maryland. Ph.D. Thesis, U. of Delaware, Newark, DE, 274 p.
- Lisle, T.E., 1989. Sediment transport and resulting deposition in spawning gravels, north coastal California. *Water Resources Research*. 26, 1303-1319.
- Macklin, M.G., Rumsby, B.T., and Heap, T., 1992. Flood alluviation and intrenchment: Holocene valley floor development and transformation in the British uplands. *Geological Society of America Bulletin*. 104, 631-643.
- McCuen, R.H., and Synder, W. M.,1985. *Hydrologic Modeling: statistical methods and applications*. Prentice-Hall, Englewood Cliffs, N.J.
- Moore, A. M. and Palmer, M.A., In press. Agricultural watersheds in urbanizing landscapes: implications for conservation of biodiversity of stream invertebrates. *Ecological Applications*.
- Packman, A.I., and McKay, J.S., 2003. Interplay of stream-subsurface exchange, clay particle deposition, and stream bed evolution. *Water Resources Research*. 39, doi:10.1029/2002WR001432.
- Palmer, M.A., Bockstael, N., Moglen, G., Wiegand, C., van Ness, K., and Pizzuto, J.,

2004. Spatial Patterning of Land Use Conversion: Linking Economics, Hydrology, and Ecology to evaluate the Effects on Stream Ecosystems. Final technical report, U.S. EPA Agreement No. R-82801021, 17 p.
- Palmer, M.A., G.E. Moglen, N. E. Bockstael, S. Brooks, J.E. Pizzuto, C. Wiegand, and K. van Ness., 2002. The ecological consequences of changing land use for running waters: the suburban Maryland case. *Yale Bulletin of Environmental Science*. 107, 85-113.
- Parker, G., 1991. Selective sorting and abrasion of river gravel. I: Theory. *Journal of Hydraulic Engineering*. 117, 131-149.
- Partheniades, E. 1986. A fundamental framework for cohesive sediment dynamics, In: Mehta, A.J. (Ed.), *Estuarine Cohesive Sediment Dynamics, Lecture Notes on Coastal and Estuarine Studies v. 14*, Springer-Verlag, Berlin, pp. 219-250.
- Rehg, K.J., Packman, A.I., and Ren, J., 2005. Effects of suspended sediment characteristics and bed sediment transport on streambed clogging. *Hydrological Processes*. 19, 413-427.
- Reid, I., and Frostick, L.E., 1985. Role of settling, entrainment and dispersive equivalence and of interstice trapping in placer formation, *Journal of the Geological Society of London*. 142, 739-746.
- Yorke, T.H., and Herb, W.J., 1978. Effects of urbanization on streamflow and sediment transport in the Rock Creek and Anacostia River Basins, Montgomery County, Maryland, 1962-1974. U.S. Geological Survey Professional Paper 1003, 71 p.
- Wilcock, P.R., 1997. The components of fractional transport rate. *Water Resources Research*. 33,247-258.

Wilcock, P.R., and Crowe, J.C., 2003. Surface-based transport model for mixed-size sediment. *Journal of Hydraulic Engineering*. 129, 120-128.

Wood, P.J., and Armitage, P.D., 1997. Biological effects of fine sediment in the lotic environment. *Environmental Management*. 21, 203-213.

More Keywords: climate change, land use, gravel-bed rivers, sediment, stream ecology, hydrology, sediment transport, fluvial geomorphology, urbanization, numerical modeling, mud, gravel, benthic habitat, sedimentation, hydraulics, global climate change, hyporheic zone, erosion, floods

Table 1. Comparison of the two climate/land-use change scenarios.

	<b>Years of Data</b>	<b>% Impervious Surface</b>	<b>% Forest</b>	<b>Buffers</b>	<b>% Construction</b>	<b>Mean Air Temp (deg. C)</b>
MG/NCC	1960-69	10	20	yes	0	17.3
US/CC	2090-99	30	2	no	2	21.5

MGN/NCC – Managed growth, no climate change

US/CC – Urban sprawl climate change scenario.

Table 2. Initial values of selected variables. Variables measured in the field are indicated, as are variables that are held constant during the simulations.

<b>Variable</b>	<b>Value (with comments)</b>
Active layer thickness (m)	0.1 (constant throughout simulation)
Fraction of bedrock in active layer	0.0275
Fraction of pores filled with mud	0.7
Bankfull depth (m)	1.0 (from field measurements)
Channel roughness length $K_s$ (m)	0.2 (calibrated to measured rating curves)
Floodplain roughness length $K_f$ (m)	0.02 (assumed)
Number of grain size fractions	10
Porosity (of mud and bed material) (%)	30 (assumed)
Sediment density ( $\text{kg/m}^3$ )	2650 (assumed)
Slope (initial)	0.0089 (from field measurements)
Shear stress below which mud settles ( $\text{N/m}^2$ )	8.72 (assumed)
Shear stress above which surface mud layers erode ( $\text{N/m}^2$ )	8.72 (assumed)
Spatial step – dx (m)	30 (assumed)
Time step (variable, max and min given)(s)	60-3000 (set to insure numerical stability)
Water density ( $\text{kg/m}^3$ )	1000
Width (bankfull)(m)	20.0 (from field measurements)
Width of floodplain (m)	200.0 (from field measurements)

## Figure Captions

Figure 1. Spatial context and geometry assumed by the model. Selected variables are also defined.

Figure 2. Empirical relationship between peak discharge ratio ( $P_R$ ) and suspended sediment concentration scaled by the mean % construction in the watershed raised to a power of 0.3. Data are illustrated for 5 watershed studied by Yorke and Herb (1978).

Figure 3. Flow duration curve comparing the frequency of discharges for the “Urban Sprawl with Climate Change” scenario with those of the “Managed Growth/No Climate Change” scenario. Flow duration curves are truncated at a frequency of 0.95. At lower frequencies, differences between the curves are indistinguishable.

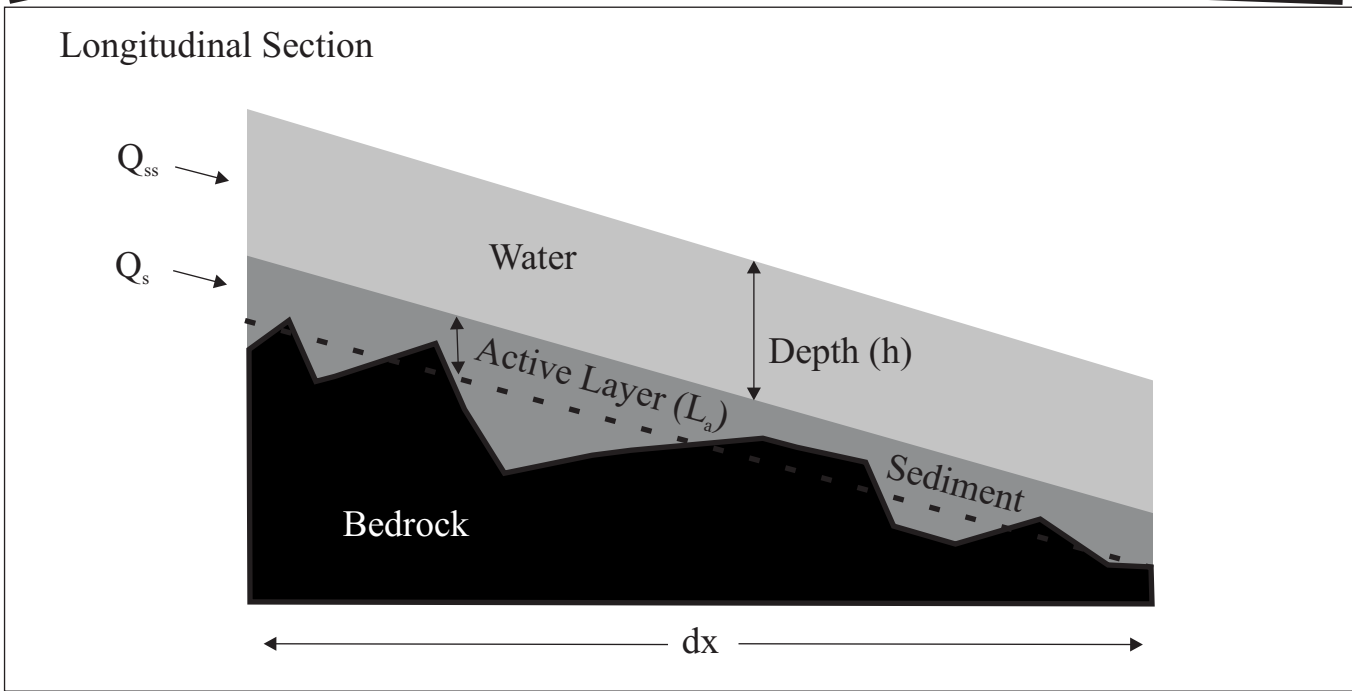
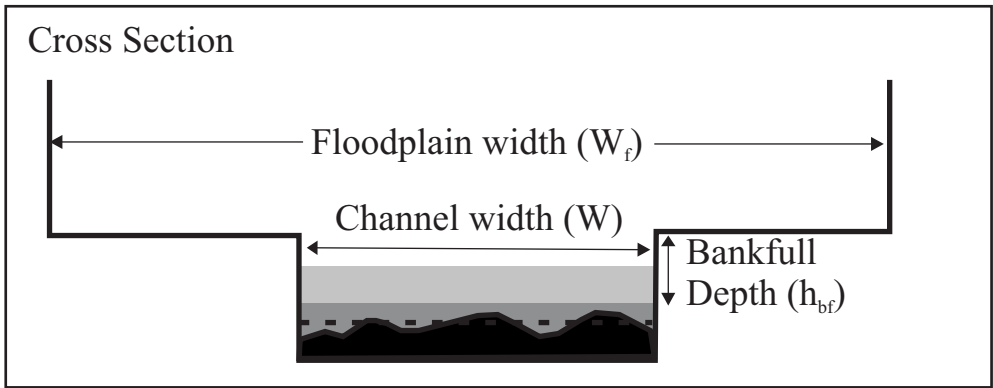
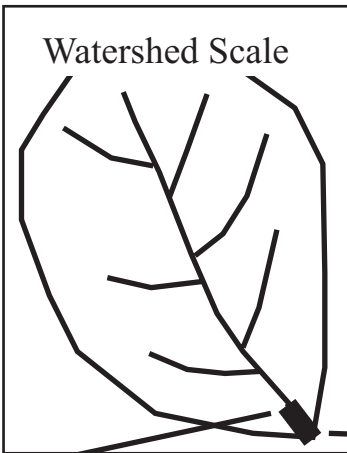
Figure 4. Duration curves for areal fraction of bed mobility for the two scenarios. The inset shows box plots for the distributions of areal bed mobility fractions for the two scenarios.

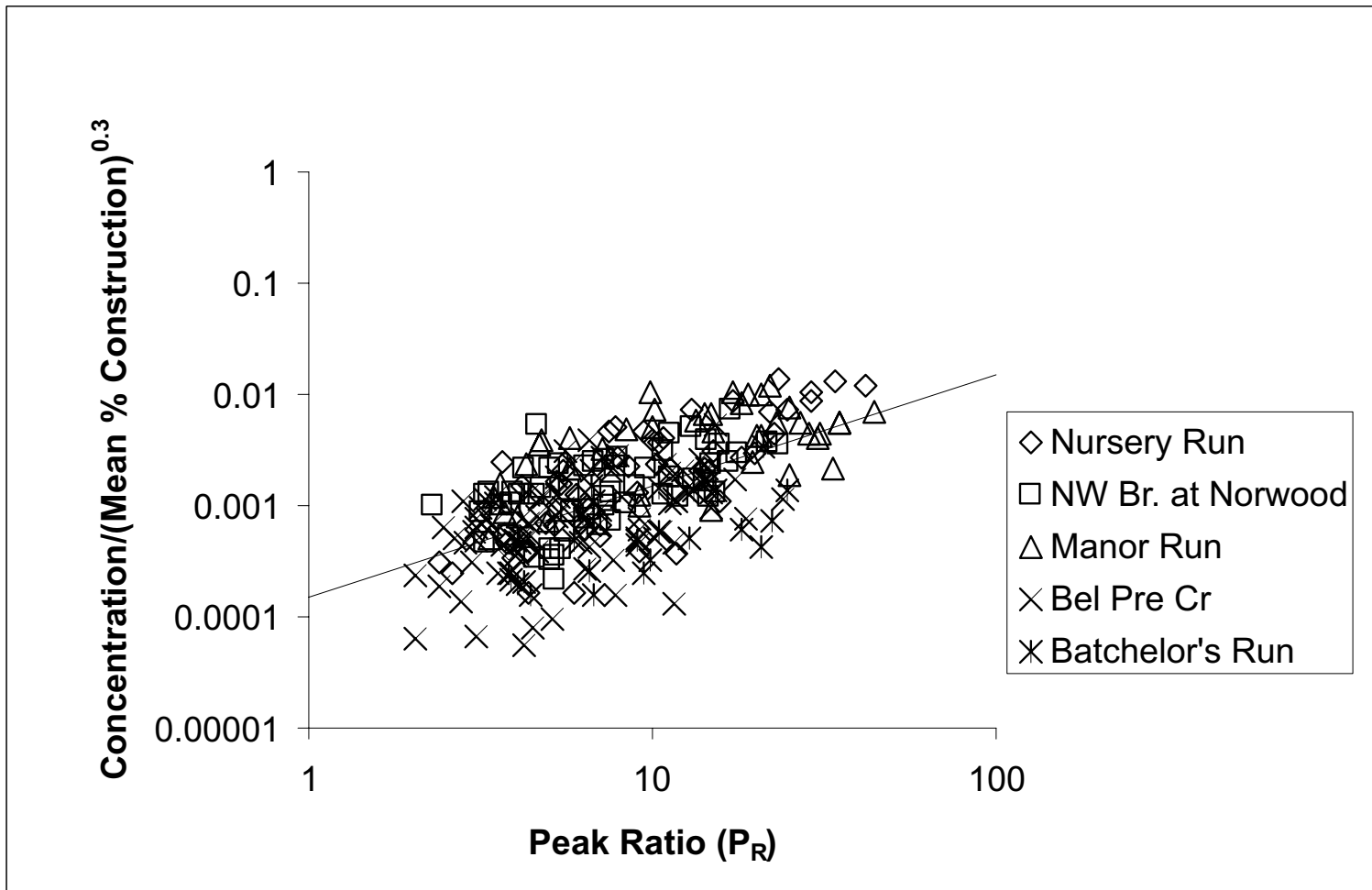
Figure 5. Time series of the fraction of exposed bedrock for the two scenarios.

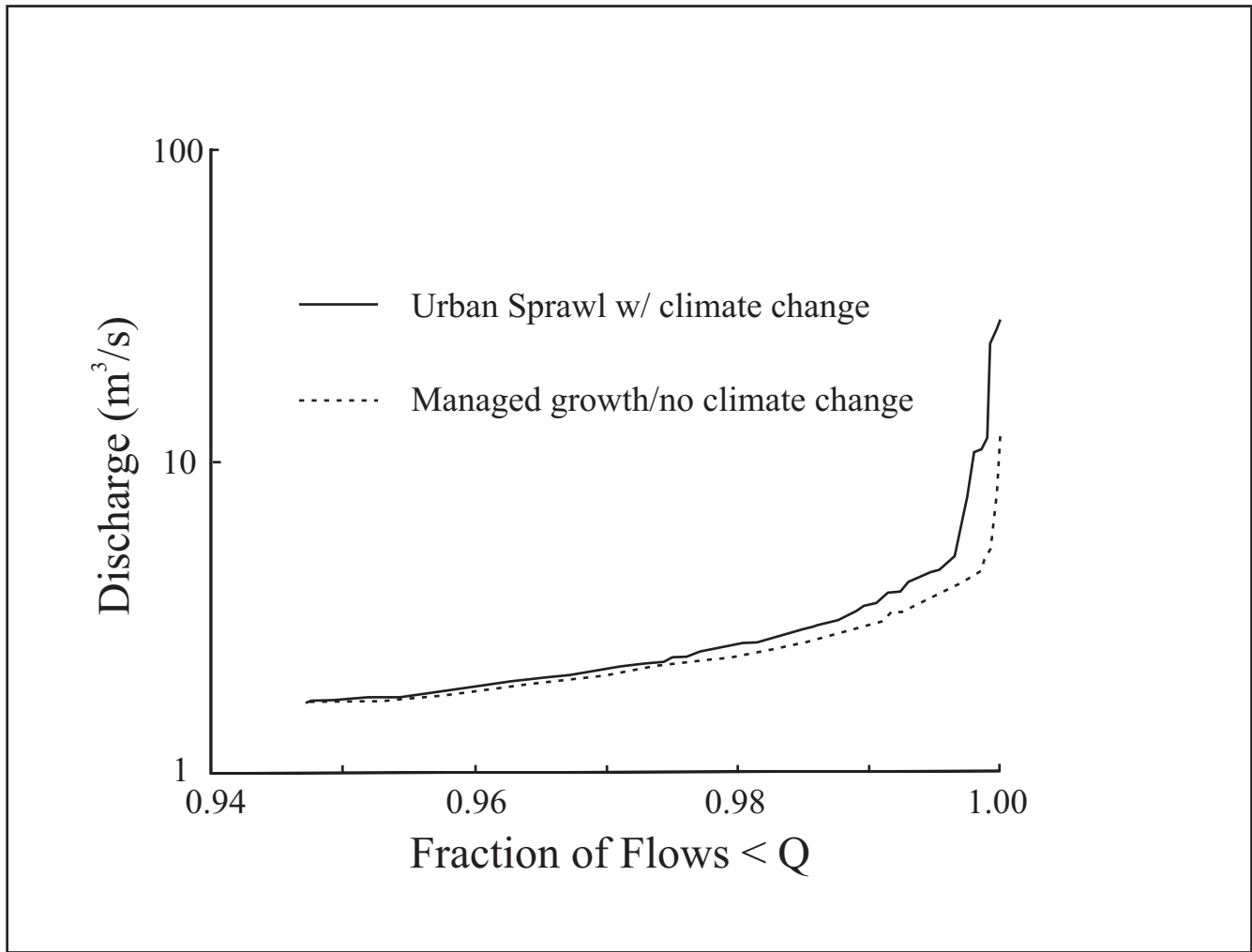
Figure 6. Duration curves for volumetric suspended sediment concentration for the two scenarios. The inset shows box plots for the distributions of sediment concentrations for the two scenarios.

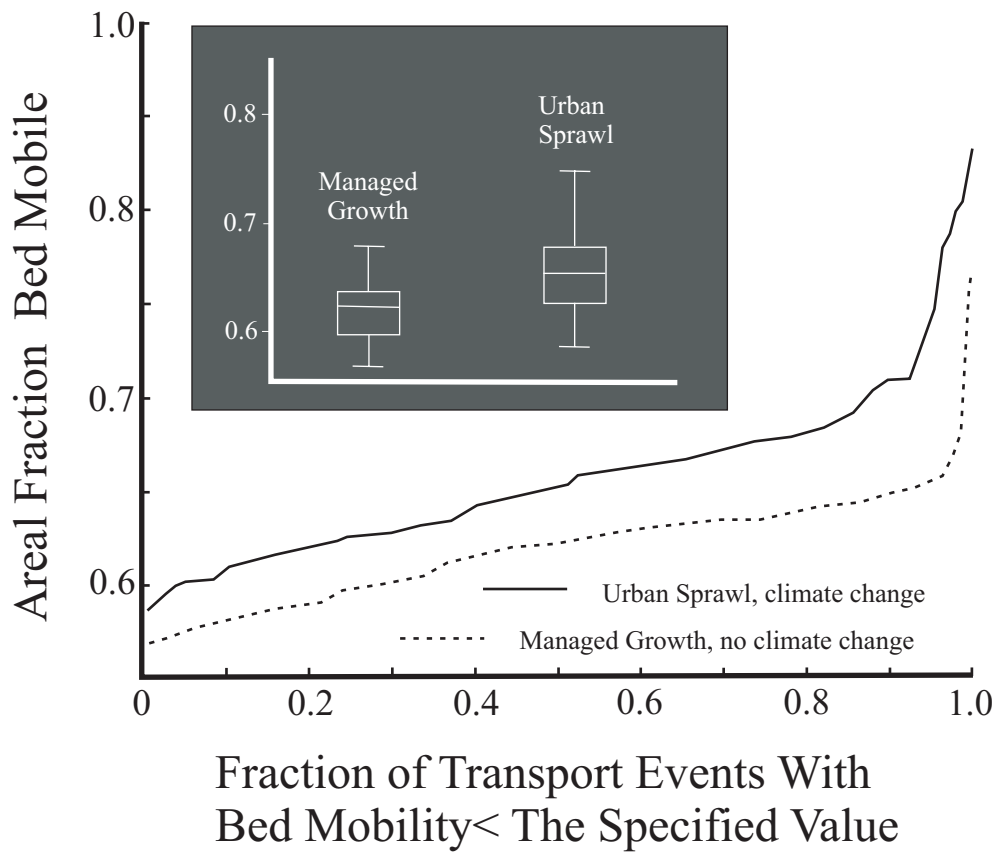
Figure 7. Time series of the fraction of pores filled with mud for the two scenarios.

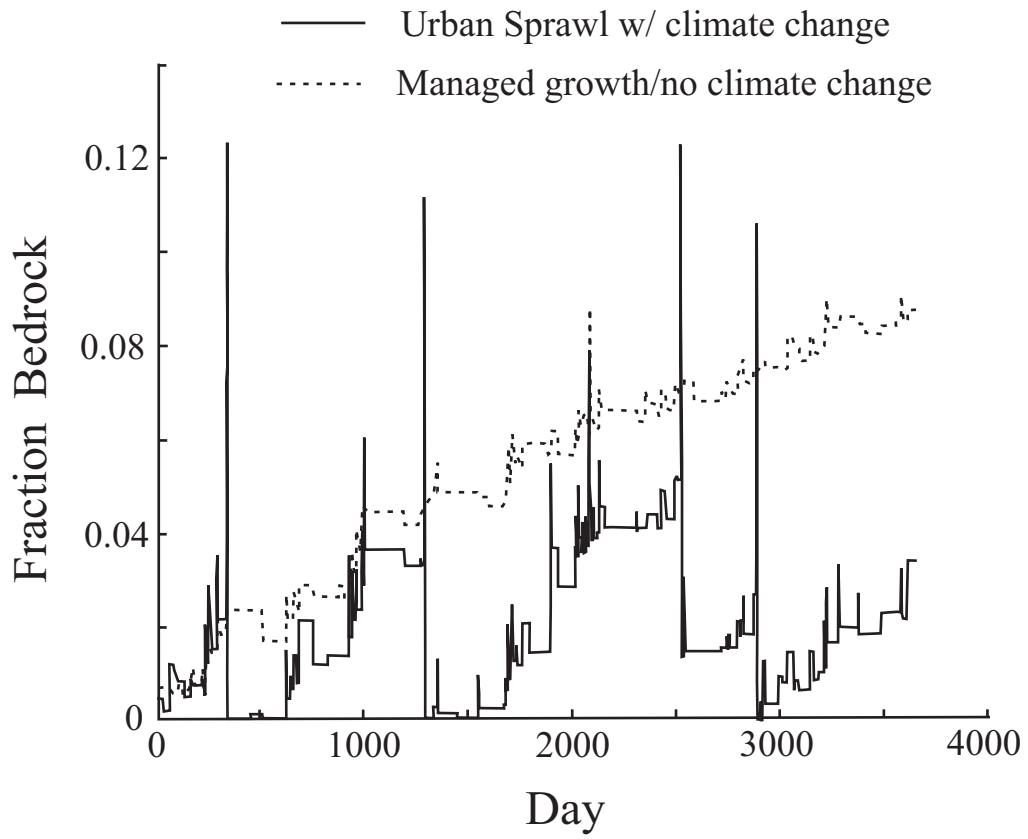
Figure 8. Results of sensitivity analyses. Percent differences from the base simulation are shown for the median and also for the 90<sup>th</sup> percentile. The sensitivity of 4 dependent variables to changes in 7 independent variables are assessed. Results are shaded according to 4 categories of sensitivity.

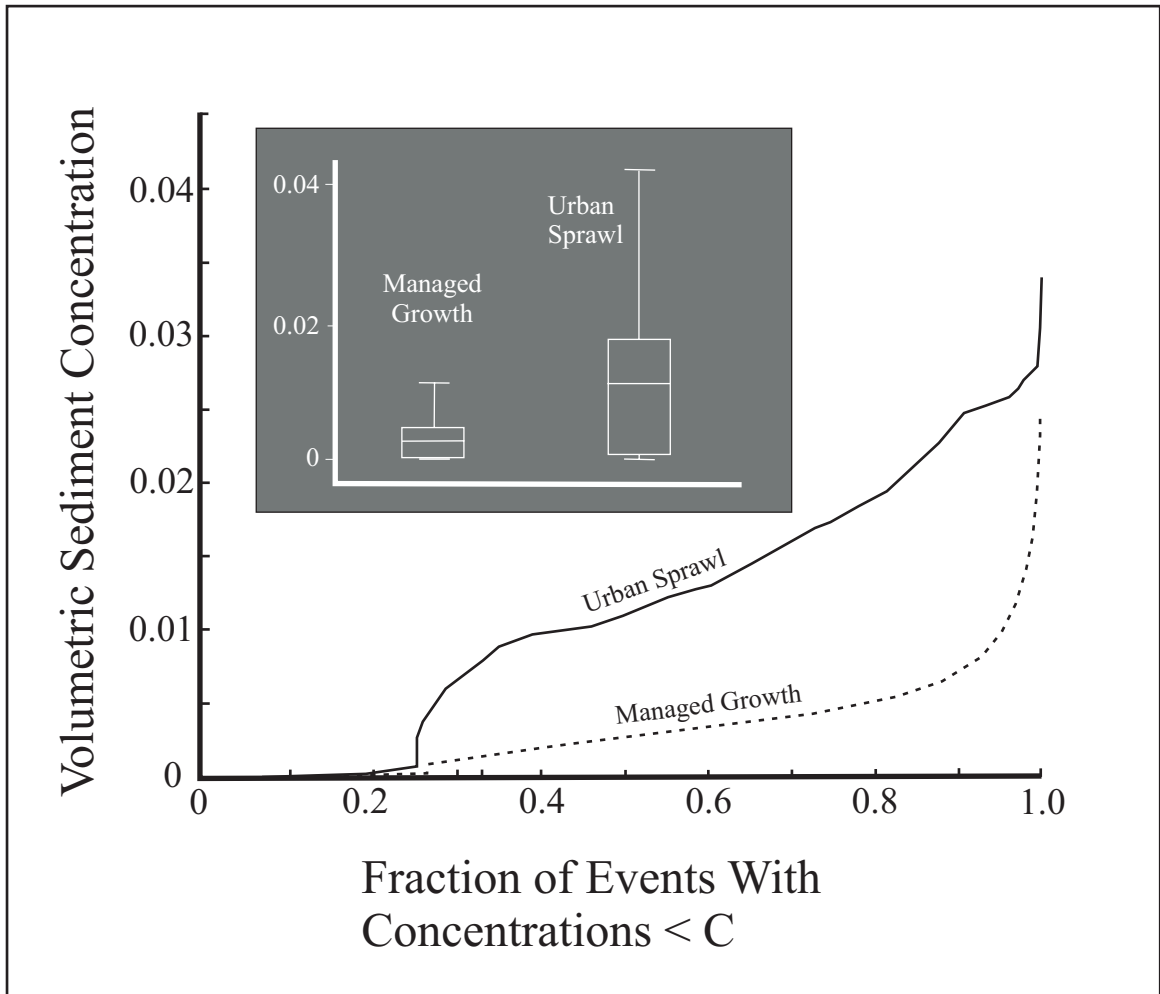


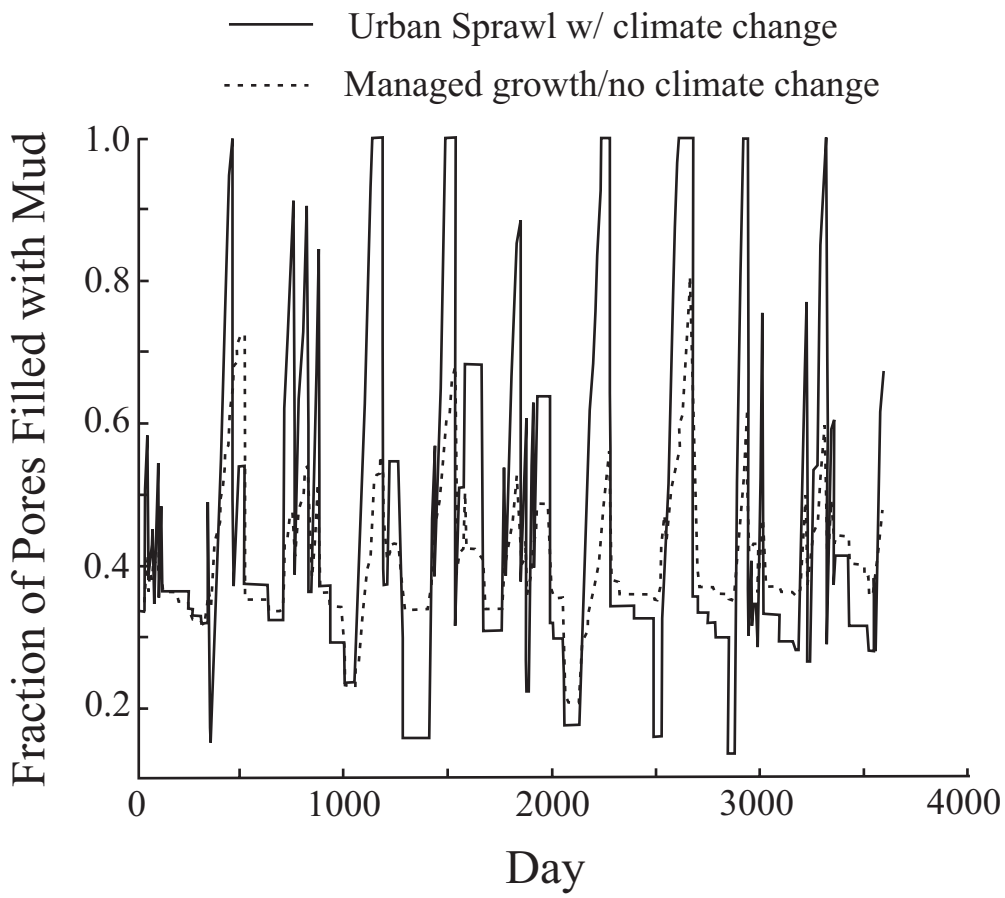












### % Changes To Median

Dep. Var. Indep. Variable	$F_{brf}$	Areal Fraction Mobile	Fraction Pores Filled With Mud	$C_m$
Q	37	-5	3	-9
$L_a$	-10	0	0	0
$K_s$	-12	-1	-14	0
$p$	0	0	0	9
$cd$	0	0	5	73
C supplied	0	0	0	82
$q_{bi}$ supplied	16171	-78	132	118

### % Changes to 90<sup>th</sup> Percentile

Dep. Var. Indep. Variable	$F_{brf}$	Areal Fraction Mobile	Fraction Pores Filled With Mud	$C_m$
Q	61	-4	-25	0
$L_a$	-7	-1	-20	0
$K_s$	-3	0	0	0
$p$	0	0	19	0
$cd$	0	0	56	42
C supplied	0	0	34	50
$q_{bi}$ supplied	4926	-51	56	4

### Legend

% Difference:	Coding
<10%	
10-25%	
25-100%	
>100%	